The Electron Storage Rings MLS and BESSY II as Primary Source Standards

Roman Klein*, Reiner Thornagel, Gerhard Ulm

Introduction

The spectral and spatial properties of the synchrotron radiation generated at electron storage rings are determined by just a few parameters and can be calculated by classical electrodynamics. In this way, electron storage rings become primary source standards [1].

Whereas the radiometric application of the black-body radiators, which can be calculated by means of Planck's radiation law, is limited to the infrared (IR), the visible, and the near-ultraviolet (UV) light, the radiation generated at electron storage rings can be applied from the THz, via the visible spectral range, to the X-ray range and – thus – opens up a spectral range for radiometric applications which is extended by several decades. PTB has been using the electron storage ring BESSY II as a primary source standard since January 1999, especially in the spectral range from the vacuum ultraviolet (VUV) to the X-ray range [2]. Furthermore – from 1984 until its shutdown in November 1999 – PTB had the electron storage ring BESSY I at its disposal as a primary source standard in the UV and the VUV spectral ranges [3, 4]. With the *Metrology Light Source* (MLS) [5, 6], PTB has, since 2008, been using a primary source standard again which is optimized for this particular spectral range.

Apart from the large spectral range, electron storage rings have another advantage: the intensity of the radiated power can be varied over many orders of magnitude via the selected number of stored electrons and can thus be adapted to the measurement requirements without changing the form of the spectrum [7]. This option of varying the electron current can be used at the MLS and at BESSY II over approx. 12 decades, however, only in special shifts which are reserved for the special operation of the respective storage ring. Furthermore, by adjusting the electron energy, the spectral shape of the synchrotron radiation emitted can be varied. This option can be used especially at the MLS.

* Dr. Roman Klein, Working Group "Synchrotron Radiation Sources", e-mail: roman.klein@ptb.de

Calculable synchrotron radiation

The radiation of relativistic electrons can be calculated by means of classical electrodynamics [1]. For the case of constant radial acceleration of relativistic electrons – as is given on the orbit in the homogeneous magnetic field of a bending magnet in an electron storage ring and is shown as an example in Figure 1 – the functional relation is described by the so-called "Schwinger theory" [8]. The spectral radiant intensity I_{0E} as a function of the photon energy E is calculated from the

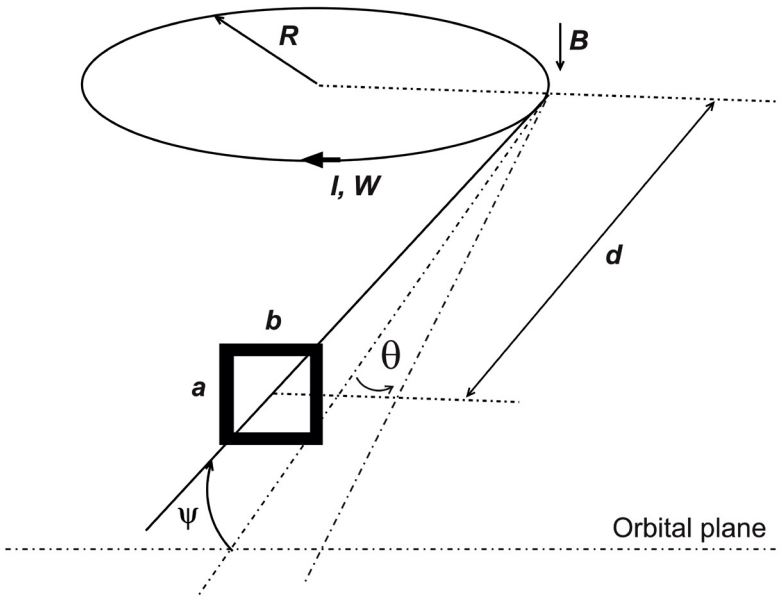

Figure 1:
Schematic representation of the parameters and of the geometry to calculate the spectral radiant power of synchrotron radiation.

magnetic induction B, the electron energy W and the electron current I by

$$I_{0E}^{\sigma} = \frac{d}{dE}\frac{d^2}{d\theta d\psi}\phi^{\sigma} = \frac{2eIR^2}{3\varepsilon_0\gamma^4}\frac{E^2}{(hc)^3}\left(\left[1+(\gamma\psi)^2\right]^2 K^2_{2/3}(\xi)\right) \quad (1)$$

for the fraction with a polarization direction (electric field vector) parallel (σ-component) to the storage ring plane and

$$I_{0E}^{\pi} = \frac{d}{dE}\frac{d^2}{d\theta d\psi}\phi^{\pi} = \frac{2eIR^2}{3\varepsilon_0\gamma^4}\frac{E^2}{(hc)^3}\left(\left[1+(\gamma\psi)^2\right](\gamma\psi)^2 K^2_{1/3}(\xi)\right) \quad (2)$$

for the fraction with a component which is vertical to it and whose phase is shifted by 90° (π-component) with

$$\xi = \frac{2\pi RE}{3hc\gamma^3}\left(1+(\gamma\psi)^2\right)^{3/2} = \frac{1}{2}\frac{E}{E_c}\left(1+(\gamma\psi)^2\right)^{3/2}$$

$$R = \frac{W}{ecB}; \quad \gamma = \frac{W}{m_0c^2} \quad .$$

Hereby, R is the radius of curvature of the electron orbit, and $K_{1/3}$ and $K_{2/3}$ are modified Bessel functions of the second kind which can be calculated numerically [9]. The angular distribution of the synchrotron radiation is homogeneous in the horizontal direction, i.e. in the orbital plane of the electrons, but is narrow in the vertical direction, where the divergence depends on the photon energy. The σ-component reaches its maximum in the orbital plane, the π-component disappears in the orbital plane.

The spectrum of the synchrotron radiation extends continuously from the far infrared into the X-ray range and is classified by the so-called "characteristic energy" E_c:

$$E_c = \frac{3hc\gamma^3}{4\pi R} \quad . \quad (3)$$

In practical units, E_c can be expressed by:

$$E_c/eV = 665.0\,B/T\,(W/GeV)^2 = 2218\,(W/GeV)^3/(R/m).$$

Eq. (1) and (2) reflect the ideal case of electrons which move exactly on the orbit. In reality, however, the electrons have a Gaussian spatial distribution around the ideal orbit, with the standard deviations σ_x and σ_y for the horizontal and the vertical directions, and an angular distribution with the standard deviations $\sigma_{x'}$ and $\sigma_{y'}$. The distribution in horizontal direction, i.e. in the orbital plane, is of no significance due to the tangential observation. The vertical distributions are summarized as follows to an effective vertical angular divergence $\Sigma_{Y'}$ for an observation point located at a distance d:

$$\Sigma_{Y'} = \left(\sigma_y{}^2/d^2 + \sigma_{y'}{}^2\right)^{1/2} \quad . \quad (4)$$

The quantity which is of interest for applications – the spectral radiant power Φ_E through an aperture of, e.g., the size $a \cdot b$ at a distance d from the source point of the radiation, can then be calculated as follows:

$$\Phi_E = \Phi_E(E;W,B,I,\Sigma_{Y'},\psi,d,a,b)$$

$$= \frac{d\Phi}{dE}(E) = \iint_{aperture}\left[\int_{-\infty}^{+\infty}\frac{1}{\sqrt{2\pi\Sigma_{Y'}}}\left[I_{0E}^{\pi}(\psi'')+I_{0E}^{\sigma}(\psi'')\right]e^{-\frac{(\psi''-\psi')^2}{2\Sigma_{Y'}^2}}d\psi''\right]d\psi' d\theta \quad . \quad (5)$$

The expressions from (1) and (2) are hence convoluted with the effective vertical beam divergence and integrated over the angular range accepted by an aperture. For a rectangular aperture as shown in Figure 1, the integration via the horizontal angle θ contributes only with a factor b/d, and in the vertical direction, the integration extends via ψ' from $(\psi - a/2d)$ to $(\psi + a/2d)$, whereby ψ is the angle of the center of the aperture (a/d, b/d, $\psi << 1$). The calculation is carried out numerically. Figure 2 and Figure 3 show the radiant power for different electron energies at the MLS and at BESSY II.

Schwinger's equation describes the special case of a relativistic electron on a circular orbit, i.e. in a homogeneous magnetic field. This condition is fulfilled for the bending magnets in an electron

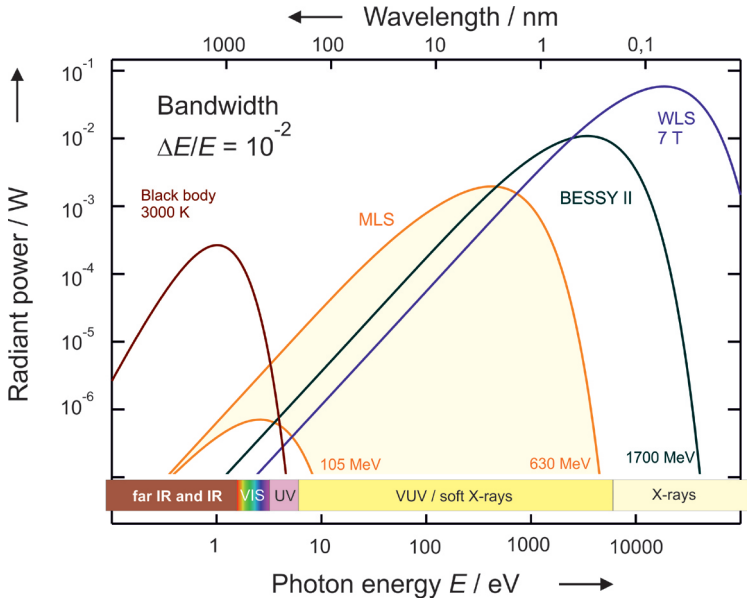

Figure 2: Calculated radiant power for some of the radiation sources utilized by PTB in comparison to a black-body radiator.

storage ring, which exhibit very good field homogeneity across the range of the radiation's source point. In addition, the radiation of an electron moving on any given trajectory can just as well be calculated by means of the formalism of classical electrodynamics. This allows the radiation of electrons to be calculated which move in magnets with strong field gradients – as is, for example, the case with *wavelength shifters* (WLS) which are operated in storage rings [10]. These WLS have a higher magnetic induction in the radiation's source point than a bending magnet and emit, according to Eq. (3), synchrotron radiation of a higher characteristic energy which can also be used for radiometric purposes. The radiation of electrons in a periodically alternating magnetic field as is given in undulators can be calculated in the same way and can be used for radiometry [11].

All quantities that enter into Eq. (5) must be known, i.e. they usually have to be measured. The relative uncertainty in the respective measured value of the quantity determines the relative uncertainty of the calculation of the spectral radiance according to Eq. (5). This will be described in more detail in the next section.

BESSY II and MLS as primary source standards

In order to be able to operate and utilize an electron storage ring as a primary source standard, the equipment of the storage ring with instruments and the storage ring operating schedule must be optimized as follows:

- The storage ring must permit stable and reproducible operation.
- Measuring devices must be installed which allow the parameters entering into eq. (5) to be determined with a sufficiently small relative uncertainty.
- The vacuum system of the storage ring (especially the vacuum chambers of the bending magnets) must be designed in such a way that the direct use of the synchrotron radiation is possible without diffraction losses, in the spectral range being of interest.
- As the spectral radiant intensity emitted by an electron storage ring under normal operating conditions is often too high for radiometric applications, and as the spatial conditions do not permit a very large distance of the calibration facility from the storage ring, the operating schedule must make it possible for the storage ring to be operated in a special operation mode, especially in the case of reduced electron beam currents. For other calibration tasks it is necessary to operate the electron storage ring at reduced electron energy in order to suppress higher monochromator diffraction orders or scattered light.

These conditions are given at BESSY II and at the MLS [1]. In the following, the measurement of the storage ring parameters and of the necessary geometrical quantities will be described in detail. For this purpose, examples from the MLS will, as far as possible, be used, which are also described in detail in [5]. Examples from BESSY II can be found in [12].

Measurement of the electron energy W

At BESSY II, the electron energy can be measured by means of two independent and complementary procedures. These procedures are resonant spin depolarization [13] and the Compton backscatter of laser photons [14, 15]. For the procedure of resonant spin depolarization, a spin-polarized electron beam is required. At BESSY II, this spin polarization builds up after approximately one hour in normal operation at an electron energy of 1.7 GeV. It can be destroyed by irradiation of radio frequency of a certain frequency. From this frequency value, the electron energy can then be calculated very precisely – in our case with a relative uncertainty of better than $5 \cdot 10^{-5}$. The spin polarization can be observed by measuring the loss rate of the stored electrons via detection of the related radiation background or via a modification of the lifetime of the electron beam current as the intrabeam scattering rate of the stored electrons exhibits a spin-dependent term. For a spin-polarized electron beam, the scattering cross section is smaller than for an unpolarized electron beam. The higher the intrabeam scattering rate of the electrons, the higher the loss rate of the stored electrons. This procedure of resonant spin depolarization is established [16]. It can, however, only be applied if the time until reaching polarization – which depends on the electron energy with the inverse of the fifth power – is in the range

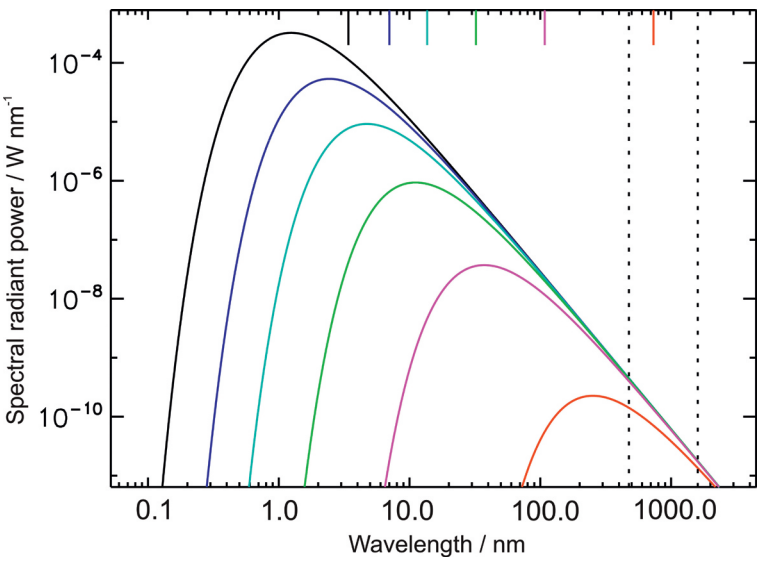

Figure 3: Calculated spectral radiant power for some electron energies of the MLS. (The calculation was carried out for the following parameters: I = 10 mA, various electron energies: W = 628 MeV, 495 MeV, 397 MeV, 299 MeV, 199 MeV and 105 MeV, from left to right, through an aperture diaphragm having a radius of r = 2.5 mm, at a distance of d = 14.8 m).

of several hours, i.e. at comparably high electron energies, as is the case at BESSY II. Therefore, the procedure of energy measurement by Compton backscattering of laser photons was established especially for the MLS [15]. For this purpose, the beam of a CO_2 laser is superimposed antiparallel to the electron beam. The laser photons scattered at the electrons in the direction of the electron beam, which now exhibit a photon energy which has been shifted by approximately $4\gamma^2$ into the very hard X-ray range, are detected with an energy-dispersive detector. From the maximum energy of the scattered photons, the electron energy can then be calculated (see Figures 4 a, b). The relative uncertainty in the determination of the electron energy amounts, with this procedure, to less than 10^{-4}. Both procedures for the determination of the electron energy were applied simultaneously – at BESSY II and at an electron energy of 1700 MeV – and showed very good agreement [15].

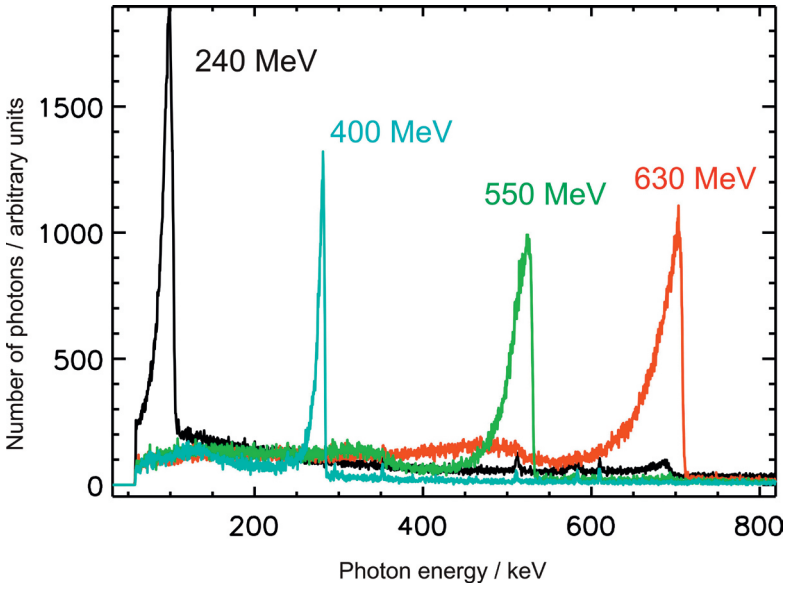

Figure 4 a:
Spectra of backscattered CO_2 laser photons for various electron energies.

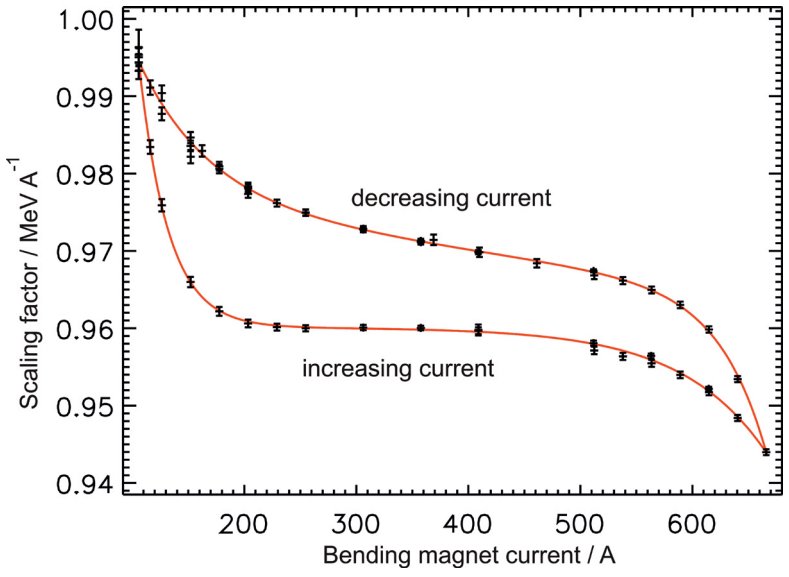

Figure 4 b:
Scaling factors between the current feed of the bending magnets and the electron energy gained by measuring the backscattered laser photons. The hysteresis of the magnets is clearly to be seen.

Measurement of the magnetic induction B at the source point

One of the bending magnets at the MLS and one of the bending magnets at BESSY II are used as sources of calculable radiation. The magnetic field of these magnets was thoroughly measured prior to the installation in order to make sure that negligibly small magnetic field gradients occur in the region of the source point. The vacuum chambers of these bending magnets are specially designed in such a way that an NMR probe can be brought to the source point of the radiation in a non-magnetic tube which can be inserted by means of a feedthrough in order to measure the magnetic induction B at the source point without a stored electron beam. The relative uncertainty for this is better than 10^{-4}.

Measurement of the electron current I

In normal user operation, the stored electron current is typically in the range of some 100 mA. PTB operates the MLS and BESSY II in special calibration shifts – in the ultimate case with only one stored electron. This corresponds to an electron beam of 1 pA at the MLS, and of 0.2 pA at BESSY II. For that reason, the instrumentation must be available to be able to adjust and measure the electron current over a range of more than 12 decades in a controllable manner. In the range of currents above 2 mA, this is done, at both storage rings, with two *Parametric Current Transformers* (PCTs) each [5].

In the range of the smallest electron currents, i.e. for currents smaller than approx. 1 nA (at the MLS) and several 100 pA (at BESSY II), the electron current is determined by counting the stored electrons and multiplying the result by the rotational frequency of the electrons [5]. For this purpose, the electrons are, after the calibration measurement has been finished, thrown out of the storage ring in a controlled way by approaching a mechanical scraper to the electron beam. At the same time, the stepwise decrease in the intensity of the radiation is observed by means of photodiodes which have been cooled down to LN2 temperature and are irradiated by the emitted synchrotron radiation (see Figure 5). In the current range lying in between, i.e. from approximately 1 nA to 2 mA, the electron current is also determined by measuring the intensity of the emitted synchrotron radiation by means of photodiodes with a linear

response behavior. Three pairs of photodiodes (one pair without filter, two pairs with filters for attenuation) are used to cover the current range described. The calibration factors which attribute an electron current to the photocurrent are then determined by comparison in the overlapping boundary area by means of the other procedures mentioned above.

Determination of the effective angular divergence $\Sigma_{Y'}$

The effective divergence of the electron beam is usually small in comparison to the vertical angular aperture of the synchrotron radiation. Therefore, the convolution of the vertical distribution of the photons with the effective divergence only brings about a small modification in the calculated spectral radiant power behind an aperture, which can be expressed by the quantity ε:

$$\Phi_E = \Phi_E\left(E; W, B, I, \Sigma_{Y'}, \psi, d, a, b\right) = \Phi_E^{Schwinger}(E; W, B, I, \psi, d, a, b) \cdot (1 + \varepsilon(E; W, B, \Sigma_{Y'}, \psi, d, a)) \quad (6)$$

whereby $\Phi_E^{Schwinger}$ is the spectral radiant power without taking the effective beam divergence into account. The quantity ε is small for typical calibration geometries and photon energies, as can be seen in Figure 6 with the example of the MLS. At BESSY II, which possesses an even smaller emittance in comparison to the MLS, the value of ε is mostly below 10^{-4} [12]. Usually, it is sufficient to calculate the value of $\Sigma_{Y'}$ from the machine parameters. These calculations are typically affected by a relative uncertainty of 20 %. Due to this, the influence in the calculation of the spectral radiant power is, however, still lower than several 10^{-4}.

Figure 7 shows measurements as examples carried out with regard to the vertical angle distribution by means of calibrated filter radiometers. For applications where the influence of the effective angle distribution has a greater influence, the effective angle distribution can also be measured by means of suitable instruments, e.g. by means of a Bragg polarimeter [17].

Measurement of the distance d from the source point and of other geometrical quantities

The source point of the synchrotron radiation is located in the vacuum chamber of the bending magnet and, thus, in the ultra-high vacuum. To measure the distance d of the source point from a flux-limiting aperture (Figure 1), an optical projection procedure is used. At a distance d_1 from the source point, a slit aperture, with slits of a well-known distance, can be inserted into the beam path. The shadow cast by this slit aperture onto a projection plane which is located at a distance d_2 from the slit aperture which has been determined very precisely by means of a laser distance meter, allows the exact determination of the distance of the projected slits and – via the intercept theorem, thus the determination of the sought total distance $d = d_1 + d_2$. By means of this method, an uncertainty of typically 2 mm is obtained.

Usually, measurements are carried out in the orbital plane, so that the vertical emission angle accounts for $\psi = 0°$. This is achieved by adjustment to the symmetry of the detector signal around the

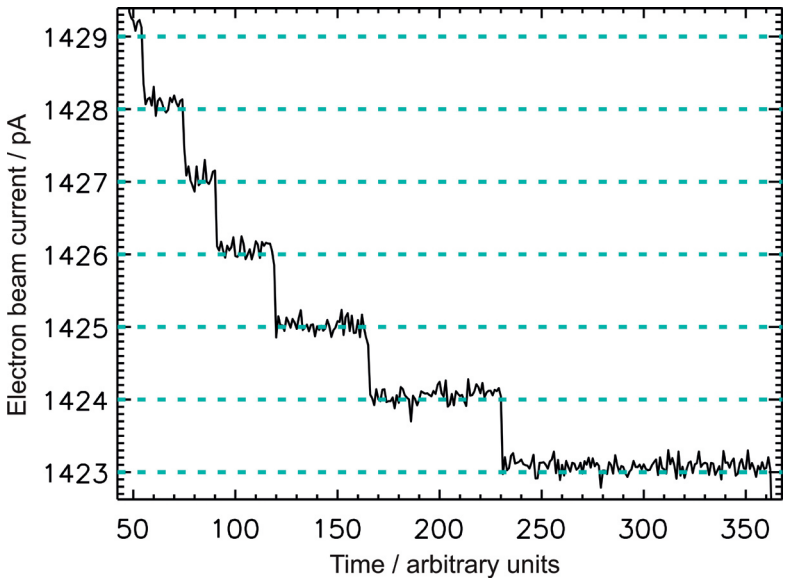

Figure 5a:
Measurement of the electron current by means of an unfiltered photodiode. Each step represents the loss of an electron.

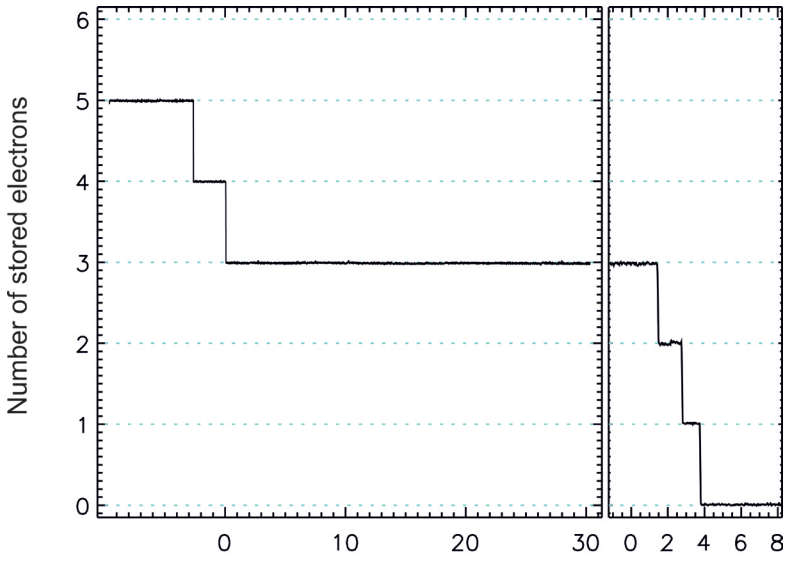

Figure 5b:
Few stored electrons with a long lifetime in the MLS (left). After the measurement, the remaining electrons are removed from the storage ring in a controllable way by means of a scraper and thereby counted.

extrema of the vertical distribution, as shown, for example, in Figure 7. A typical adjustment error lies in the range of some µrad.

The quantity $a \cdot b$ of a flux-limiting aperture diaphragm is determined geometrically, e.g. by means of a measuring microscope. As the aperture diaphragm is usually a detector property, the uncertainty in its determination is not attributed to the primary source standard, but to the detector.

Uncertainties and comparison with other standards

In Table 1, the uncertainties in the determination of the input parameters of the Schwinger formula

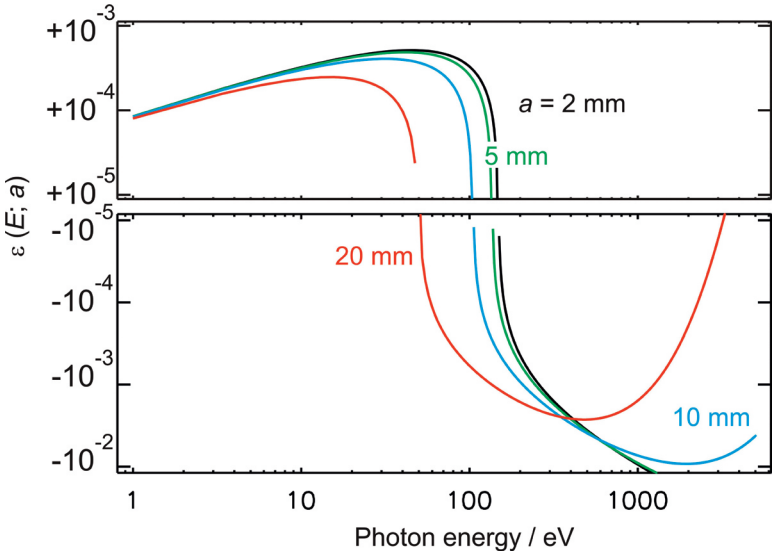

Figure 6:
Influence of the quantity ε on the spectral radiant power at the MLS through an aperture at a distance d = 15 m for various vertical aperture diaphragms a (W = 600 MeV; B = 1.3 T; Σ_V' = 50 µrad, ψ = 0 mrad).

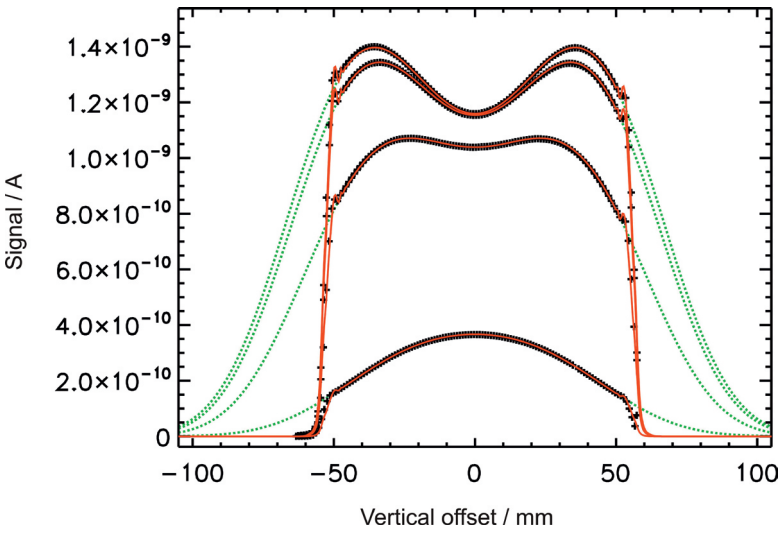

Figure 7:
Calculated (red) and measured vertical distribution (+) of the synchrotron radiation at 476 nm for various electron energies of the MLS (from above: 628 MeV, 397 MeV, 199 MeV, 105 MeV).

are summarized for the MLS and for BESSY II. The respective influence of the uncertainty of these parameters on the overall uncertainty of the calculation of the spectral radiant power depends on the photon energy and was calculated by the numerical partial derivative [5]. Up to photon energies of approximately the characteristic energy, the relative uncertainty remains almost constant at small values and is dominated by the distance measurement and by the current measurement. For higher photon energies, it then increases strongly and is mainly dominated by the uncertainty in the determination of the magnetic induction in the source point and of the electron energy. The smallest relative uncertainties can thus be realized for photon energies below the characteristic energy, so that it may be of advantage for measurements at high photon energies to use a source with a higher characteristic energy – such as, e.g., a superconducting wavelength shifter [10]. If you compare, however, the uncertainty in the calculation at certain photon energies with the radiant power available at these photon energies, especially compared to the overall radiated power, it becomes clear that, in the case of certain calibration procedures, limitations arise in the utilizable spectral range. This applies, e.g., in the case of the source-based calibration of radiation sources [18, 33], i.e. in the direct comparison of the radiation properties of an unknown source with those of the primary source standard by means of wavelength-dispersive monochromator detector systems. Here, higher diffraction orders of the monochromator cause high uncertainties in the calibration if the measurements are carried out at low photon energies and – thus – low available radiant power, in comparison with the higher energetic fraction of the spectrum. Here, an operation – e.g. of the MLS – at reduced electron energy then becomes necessary.

Since using synchrotron radiation for radiometric purposes began, the spectral radiant intensity of electron storage rings which are operated as primary source standards has been compared with other established source standards or detector standards. These comparisons serve to verify the realized radiometric scales and to validate the uncertainty budget.

For example, the primary standards "electron storage ring" and "black-body radiator" were compared by several working groups by means of transfer radiators (tungsten filament lamps) or filter radiometers in the range of the spectral overlap between synchrotron radiation and black-body radiation, i.e. in the spectral range of the IR and of the VIS [3, 19, 20, 21]. The primary source standard BESSY I was compared to a cryogenic radiometer as the primary detector standard, both spectrally, by means of filter radiometers [21, 22, 23], and

MLS		$\Delta\Phi(E)/\Phi(E)$ *10^{-3} ($k=1$) at E =		
Parameters	**Value**	1 eV	100 eV	1000 eV
Electron energy W	600.00(6) MeV	0.07	0.12	0.67
Magnetic induction B	1.30000(13) T	0.07	0.04	0.27
Electron current I	100.00(2) mA	0.20	0.20	0.20
Eff. vert. divergence $\Sigma_{Y'}$	44(9) µrad	0.04	0.18	1.5
Vert. emission angle ψ	0(5) µrad	0.0007	0.003	0.03
Distance d	15000(2) mm	0.27	0.26	0.17
Total		0.35	0.40	1.7
BESSY II		$\Delta\Phi(E)/\Phi(E)$ *10^{-3} ($k=1$) at E =		
Parameters	**Value**	1 eV	100 eV	1000 eV
Electron energy W	1718.60(6) MeV	0.1	0.3	1.4
Magnetic induction B	1.29932(12) T	0.06	0.3	1.8
Electron current I	10.000(2) mA	0.2	0.2	0.2
Eff. vert. divergence $\Sigma_{Y'}$	3.5(7) µrad	0.06	0.2	0.4
Vert. emission angle ψ	0(2) µrad	0.04	0.2	0.3
Distance d	30 000(2) mm	0.1	0.1	0.1
Total		0.3	0.6	2.3

Tab. 1: Sample parameter set for the calculation of the spectral radiant power of the MLS and of BESSY II according to Schwinger, including uncertainties in the determination of the parameters.

by measuring the emitted overall radiant power by means of the detector standard [24]. The two primary standards BESSY I and BESSY II were compared in the range of the UV and VUV by means of deuterium lamps as transfer radiators [25], and in the X-ray range by means of a Si(Li) detector as a transfer detector [26]. Furthermore, the primary source standard BESSY I was compared with radioactive standards [27] in the X-ray range at 6.4 keV and 8.0 keV by means of a Si(Li) detector. By means of deuterium lamps as transfer standards, a comparison between BESSY II and the SURF-III electron storage ring of NIST took place [28]. At the MLS, a comparison at different electron energies was carried out with filter radiometers which were calibrated traceably to a cryogenic radiometer as the primary detector standard (Figures 7, 8) [29]. Furthermore, the emitted overall radiant power was measured by means of a cryogenic radiometer at the MLS for a large set of parameters with various electron energies and electron beam currents (Figure 9) [30].

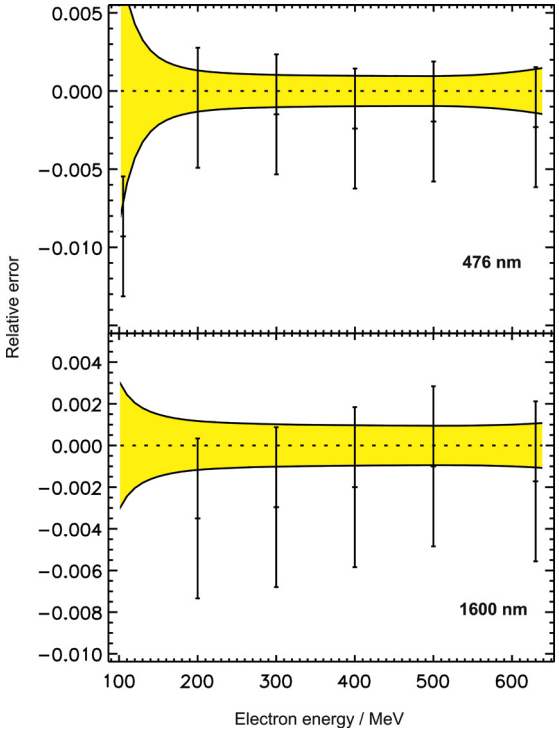

Figure 8: Comparison of the calculated radiant intensity of the MLS with the radiant intensity measured by means of calibrated filter radiometers at 476 nm and 1600 nm for various electron energies.

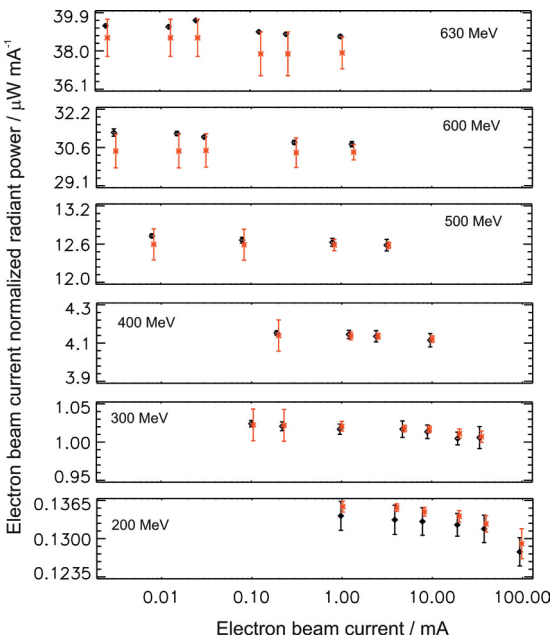

Figure 9: Comparison of the radiant power calculated from the storage ring parameters (red) with the radiant power measured by means of a cryogenic radiometer (black) for various electron energies and electron currents of the MLS.

For all these comparisons in the IR, VIS, UV, VUV, EUV and X-ray ranges, a good agreement became evident whose uncertainty was not determined by the realization of the unit by means of the source standard, but by the comparison procedure or by the transfer standards used.

Summary and applications

The electron storage rings MLS and BESSY II are established as national primary source standards in the spectral range of the visible up to the X-ray ranges. The relative uncertainty of the realization of the spectral radiant power amounts, in the major part of the covered spectral range, to less than 0.1 %. The undispersed radiation can be used for the direct calibration of energy-dispersive detectors such as *high-purity germanium* (HPGe), Si(Li) or SSD detectors, or for the calibration of wavelength-dispersive spectrographs – as is envisaged, for example, for the calibration of the SPICE spectrograph [31] of the Solar Orbiter Mission [32]. Furthermore, radiation sources can be traceably calibrated to the respective primary source standard [33] by means of a wavelength-dispersive transfer system. At the MLS, a new measuring set-up has been put into operation for this purpose which covers the spectral range from 7 nm to 400 nm [34, 35].

The high dynamics in the radiant intensity, and the possibility of exact determination, also allow the building of a radiation-metrological bridge from conventional radiometry to single-photon radiometry. In this connection, a single-photon detector was, for example, traceably calibrated to a cryogenic radiometer at the MLS [36].

References

[1] *J. Hollandt, J. Seidel, R. Klein, G. Ulm, A. Migdall, M. Ware*: in Optical Radiometry, A. C. Parr, R. U. Datla, J. L. Gardner (Eds.), 213–290, Elsevier, Amsterdam (2005)

[2] *R. Thornagel, R. Klein, G. Ulm*: Metrologia **38**, 385 (2001)

[3] *F. Riehle, B. Wende*: Opt. Lett. **10**, 365 (1985)

[4] *F. Riehle, B. Wende*: Metrologia **22,** 75 (1986)

[5] *R. Klein et al.*: Phys. Rev. ST Accel. Beams **11**, 110701 (2008)

[6] *R. Klein, G. Brandt, R. Fliegauf, A. Hoehl, R. Müller, R. Thornagel, G. Ulm*: Metrologia **46**, S266 (2009)

[7] *R. Klein, R. Thornagel, G. Ulm*: Metrologia **47**, R33 (2010)

[8] *J. Schwinger*: Phys. Rev. **75**, 1912 (1949)

[9] *V. O. Kostroun*: Nucl. Instr. and Meth. **172**, 371 (1980)

[10] *R. Klein, G. Brandt, L. Cibik, M. Gerlach, M. Krumrey, P. Müller, G. Ulm, M. Scheer*: Nucl. Instr. and Meth. **580**, 1536 (2007)

[11] *K. Molter, G. Ulm*: Rev. Sci. Instrum. **63**, 1296 (1992)

[12] *R. Klein, R. Thornagel, G. Ulm*: PTB-Mitteilungen **115**, No. 3, 8 (2005)

[13] *P. Kuske, R. Goergen, R. Klein, R. Thornagel, G. Ulm*: Proc. EPAC 2000, 1771 (2000)

[14] *R. Klein, T. Mayer, P. Kuske, R. Thornagel, G. Ulm*: Nucl. Instr. and Meth. A **384**, 293 (1997)

[15] *R. Klein, P. Kuske, R. Thornagel, G. Brandt, R. Görgen, G. Ulm*: Nucl. Instr. and Meth. A **486**, 541 (2002)

[16] *A. Lysenko, I. Koop, A. Polunin, E. Pozdeev, V. Ptitsin, Yu. Shatunov*: Nucl. Instr. and Meth. A **359,** 419 (1995)

[17] *R. Klein, G. Brandt, R. Thornagel, J. Feikes, M. Ries, G. Wüstefeld*: Proc. IPAC 2011, 1165 (2011)

[18] *M. Richter, J. Hollandt, U. Kroth, W. Paustian, H. Rabus, R. Thornagel, G. Ulm*: Metrologia **40**, S107 (2003)

[19] *A. R. Schaefer, R. D. Saunders, L. R. Hughey*: Opt. Eng. **25**, 892 (1986)

[20] *H. J. Kostkowski, J. L. Lean, R. D. Saunders, L. R. Huhgey*: Appl. Opt. **25**, 3297 (1986)

[21] *M. Stock, J. Fischer, R. Friedrich, H. J. Jung, R. Thornagel, G. Ulm, B. Wende*: Metrologia **30**, 439 (1993)

[22] *N. P. Fox, P. J. Key, F. Riehle, B. Wende*: Appl. Opt. **25**, 2409 (1986)

[23] *R. Thornagel, J. Fischer, R. Friedrich, M. Stock, G. Ulm, B. Wende*: Metrologia **32**, 459 (1995/96)

[24] *H. Rabus, R. Klein, F. Scholze, R. Thornagel, G. Ulm*: Metrologia **39**, 381 (2002)

[25] *M. Richter, J. Hollandt, U. Kroth, W. Paustian, H. Rabus, R. Thornagel, G. Ulm*: Metrologia **40**, 107 (2003)

[26] *F. Scholze, R. Thornagel, G. Ulm*: Metrologia **38**, 391 (2001)
[27] *D. Arnold, G. Ulm*: Nucl. Instr. and Meth. A **339**, 43 (1994)
[28] *U. Arp, R. Klein, Z. Li, W. Paustian, M. Richter, P.-S. Shaw, R. Thornagel*: Metrologia **48**, 261 (2011)
[29] *R. Klein, D. Taubert, R. Thornagel, J. Hollandt, G. Ulm*: Metrologia **46**, 359 (2009)
[30] *R. Klein, A. Gottwald, G. Brandt, R. Fliegauf, A. Hoehl, U. Kroth, H. Kaser, M. Richter, R. Thornagel, G. Ulm*: Metrologia **48**, 219 (2011)
[31] *A. Fludra et al.*: Proc. SPIE **8862**, 88620F (2013)
[32] *A. Gottwald, R. Klein, M. Krumrey, P. Müller, W. Paustian, T. Reichel, F. Scholze, R. Thornagel*: in this publication on p. 30
[33] *R. Klein, R. Fliegauf, S. Kroth, W. Paustian, M. Richter, R. Thornagel*; in this publication on p. 16
[34] *R. Thornagel, R. Klein, S. Kroth, W. Paustian, M. Richter*: **51** Metrologia, 528 (2014)
[35] *R. Thornagel, R. Fliegauf, R. Klein, S. Kroth, W. Paustian, M. Richter*: Rev. Sci. Instr. **86**, 013106 (2015)
[36] *I. Müller, R. M. Klein, J. Hollandt, G. Ulm, L. Werner*: Metrologia **49**, S152 (2012)